Molecular Plant Pathology

MOLECULAR PLANT PATHOLOGY (2018) 19(4), 961–974 DOI: 10.1111/mpp.12582

The transcription factor *PstSTE12* is required for virulence of *Puccinia striiformis* f. sp. *tritici*

XIAOGUO ZHU†, WEI LIU†, XIULING CHU, QIXIONG SUN, CHENGLONG TAN, QIAN YANG, MIN JIAO, JUN GUO* AND ZHENSHENG KANG*

State Key Laboratory of Crop Stress Biology for Arid Areas, College of Plant Protection, Northwest A&F University, Yangling, Shaanxi 712100, China

SUMMARY

Puccinia striiformis f. sp. *tritici* (*Pst*) is an obligate biotrophic fungus that causes extensive damage in wheat. The pathogen is now known to be a heteroecious fungus with an intricate life cycle containing sexual and asexual stages. Orthologues of the *STE12* transcription factor that regulate mating and filamentation in *Saccharomyces cerevisiae*, as well as virulence in other fungi, have been extensively described. Because reliable transformation and gene disruption methods are lacking for *Pst*, knowledge about the function of its STE12 orthologue is limited. In this study, we identified a putative orthologue of *STE12* from *Pst* in haustoria-enriched transcripts and designated it as *PstSTE12*. The gene encodes a protein of 879 amino acids containing three helices in the homeodomain, conserved phenylalanine and tryptophan sites, and two C_2/H_2-Zn^{2+} finger domains. Real-time reverse transcription-polymerase chain reaction (RT-PCR) analyses revealed that the expression of *PstSTE12* was highly induced during the early infection stages and peaked during haustorium formation and the pycniospore stage in the aecial host barberry. Subcellular localization assays indicated that *PstSTE12* is localized in the nucleus and functions as a transcriptional activator. Yeast one-hybrid assays revealed that PstSTE12 exhibits transcriptional activity, and that its C-terminus is necessary for the activation of transcription. *PstSTE12* complemented the mating defect in an α *ste12* mutant of *S. cerevisiae*. In addition, it partially complemented the defects of the *Magnaporthe oryzae mst12* mutant in plant infection. Knocking down *PstSTE12* via host-induced gene silencing (HIGS) mediated by *Barley stripe mosaic virus* (BSMV) resulted in a substantial reduction in the growth and spread of hyphae in *Pst* and weakened the virulence of *Pst* on wheat. Our results suggest that *PstSTE12* probably acts at an intersection participating in the invasion and mating processes of *Pst*, and provide new insights into the comprehension of the variation of virulence in cereal rust fungi.

Keywords: mating, *Puccinia striiformis* f. sp. *tritici*, STE12, virulence.

* *Correspondence*: Email: guojunwgq@nwsuaf.edu.cn; kangzs@nwsuaf.edu.cn

†These authors contributed equally to this work.

INTRODUCTION

Wheat stripe rust, caused by *Puccinia striiformis* f. sp. *tritici* (*Pst*), is a serious threat to worldwide wheat production and global food security (Kolmer, 2005). Yield losses of more than 90% in a single crop season caused by *Pst* have been reported in many countries (Chen, 2014; Line, 2002; Roelfs and Bushnell, 1985; Wellings, 2011). Despite the importance of *Pst*, the intricate life cycle has impeded the pursuit of the dissection of pathogenesis in this pathogen. As a strict obligate biotrophic fungus, *Pst* cannot survive without living tissue from cereal crops to provide nutrition (Eugenea *et al.*, 2009). In addition, stripe rust fungi require an alternative host barberry to complete the macrocyclic sexual life cycle (Jin *et al.*, 2010; Zhao *et al.*, 2013). In general, barberry enables rust fungi to survive winter, provides initial inoculum to cereal crops, generates new races and confers diversification of rust populations (Zhao *et al.*, 2016). The urediniospores are usually produced early in the next growing season and dispersed as airborne inoculum to produce new infections in vegetative tissues of the host plant. This cycle is repeated many times, often causing epidemics in the wheat crop (Eugenea *et al.*, 2009; Kolmer, 2005). This complex life cycle, especially the sexual stage, has contributed to the high degree of virulence diversity in *Pst*, which can enhance its pathogenicity, increase its host range and generate new physiological races through sexual hybridization (Wang and Chen, 2013; Zheng *et al.*, 2013). Therefore, sexual reproduction plays a critical role in *Pst*, as well as virulent urediniospores.

Previous studies have shown that many genes perform biochemical or physiological functions involved in sexual and asexual reproduction, including transcription factors (TFs), which interact with different DNA-binding domains (Min *et al.*, 2012; Son *et al.*, 2011) and key conserved components of signal transduction pathways (Johnson, 1995; Urban *et al.*, 2003; Yang *et al.*, 2015; Zhou *et al.*, 2011). Mitogen-activated protein (MAP) kinase cascades, as essential signalling pathways, have attracted considerable research attention because of their broadly conserved roles in a variety of fungi, plants and mammals (Hamel and Ellis, 2012). In *Saccharomyces cerevisiae*, the filamentation invasion pathway and mating pathway are controlled by FUS3 and KSS1, which are MAP kinases (Madhani and Fink, 1997). Activation by mating pheromones occurs only in cells containing a STE12/DIG1/DIG2 complex. The FUS3- or KSS1-mediated phosphorylation of STE12

relieves their inhibitory activity through two elementary proteins, DIG1 and DIG2 (Chou *et al.*, 2006; Schamber *et al.*, 2010). In contrast, the TEC1/STE12/DIG1 complex, containing the TF TEC1, is known to be involved in the activation of genes that determine filamentation formation (Chou *et al.*, 2006). Although the activation of the two pathways depends on different activation mechanisms and components, they share the downstream TF STE12 as a central node to respond to mating as well as invasive growth (Madhani and Fink, 1997).

STE12-like TFs showing similarities to yeast *STE12* have been identified in many true filamentous fungi and play essential roles in sexual development and pathogenicity (Hoi and Dumas, 2010). These proteins contain two C-terminus-located, tightly linked, C_2H_2 zinc fingers, which are absent in yeast STE12. Currently, the role of the C_2H_2 domain is still unclear. Deletion of this domain does not impair DNA binding *in vitro* (Chang *et al.*, 2004; Hoi *et al.*, 2007), but, *in vivo*, the integrity of this domain is required for the function of the protein in *Colletotrichum lindemuthianum* and *Magnaporthe oryzae* (Hoi *et al.*, 2007; Park *et al.*, 2004). The saprophytic *Neurospora crassa STE12*-like *pp-1* mutant shows a severe reduction in the growth rate and production of aerial hyphae, and fails to develop protoperithecia (Li *et al.*, 2005). A similar phenotype has been observed for the MAP kinase *mak-2* mutant, suggesting that *pp-1* in *N. crassa* is controlled by this MAP kinase pathway. In hemibiotrophic fungal pathogens, *C. lindemuthianum CLSTE12* may be involved in the production of cell surface proteins and host cell wall-degrading enzymes (Hoi *et al.*, 2007). In plant pathogens, *M. oryzae STE12* orthologous genes are important for the development of specialized infectious structures, including appressoria, for the penetration of leaf surfaces and subsequent invasive growth. *STE12*-deficient mutants are defective in penetration and either non-pathogenic or strongly reduced in virulence (Kramer *et al.*, 2009; Park *et al.*, 2002). Similar functions for *STE12* have also been documented in the basidiomycete yeast *Cryptococcus neoformans*, which is an important human fungal pathogen (Chang *et al.*, 2001; Yue *et al.*, 1999). Deletion of *STE12* in both *MATa* and *MATα* strains affects the mating efficiency and markedly reduces the virulence in mice. From previous studies, almost all *STE12* and *STE12*-like factors play key roles in the regulation of fungal development and pathogenicity (Hoi and Dumas, 2010; Rispail and Pietro, 2010); however, their roles in sexual development cannot be ascribed for all fungi, e.g. the *M. oryzae mst12* mutation has no effect on sexual development (Park *et al.*, 2002).

Although *STE12* orthologues have been reported to be involved in various cellular processes in many pathogens (Hoi and Dumas, 2010; Hoi *et al.*, 2007; Rispail and Di, 2009; Schamber *et al.*, 2010), the role of *STE12* in *Pst* is still unknown. In a previous study, RNA sequencing (RNA-seq) analysis indicated that sequences with homology to the *STE12*-like gene (PST79_9215) were found in both haustoria and germinated spores of *Pst* and the encoded proteins with functions were related to TF activity (Garnica *et al.*, 2013). Subsequently, three pheromone receptor (*STE3*) mating-type genes, together with two allelic homeodomain (HD) pairs (*HD1* and *HD2*), were identified in each dikaryotic *Puccinia* species. The HD proteins were active during mating through heterologous expression in *Ustilago maydis*, and host-induced gene silencing (HIGS) of the *HD* and *STE3* genes reduced infection in wheat (Cuomo *et al.*, 2016). In this study, we report our findings on the characterized mating-related gene from *Pst*, *PstSTE12*, which was identified by transcriptome sequencing. To clarify whether and how *PstSTE12* participates in the mating and virulence of *Pst*, we performed sequence analysis, subcellular localization, transcriptional activation analyses, complementation of mutants of *S. cerevisiae* and *M. oryzae*, and *PstSTE12* knockdown via HIGS. Our findings suggest that *PstSTE12* is an important TF responsible for *Pst* virulence, and may be involved in the mating process, providing insights into virulence variation in cereal rust fungi.

RESULTS

A highly induced gene in *Pst* haustoria is identified as a *STE12* gene

To find novel pathogenicity factors and to identify haustoria-enriched transcripts in *Pst*, we performed RNA-seq analysis with haustoria isolated from wheat Suwon 11 (Su11) leaves infected with the virulent *Pst* isolate CYR32. One of the transcript sets that encodes a putative fungal TF was identified in the resulting RNA-seq data. Mapping to the CYR32 genome (Zheng *et al.*, 2013) showed that it encodes a putative STE12 involved in the MAP kinase pathway. We designated this gene *PsSTE12*. *PstSTE12* has an open reading frame of 2637 bp encoding a protein of 879 amino acids and containing three conserved HD kinase domains. N-terminal residues of PstSTE12 indicate significant identity to other STE12 proteins (Fig. S1A, see Supporting Information), and this region includes three conserved HDs from residues 106–199 of PstSTE12, based on the *S. cerevisiae* STE12 sequence. *Saccharomyces cerevisiae* STE12 contains the DNA recognition domain for the binding of pheromone response elements with HD-Helix III (Vallim *et al.*, 2000; Yuan and Fields, 1991). As shown in Fig. S1A, this helix exhibits high conservation amongst these fungi, and PstSTE12 contains the universally conserved tryptophan (residue 95) followed by the phenylalanine of Helix III believed to be essential for DNA binding. Amino acid identity over this region is 86%, 88%, 62%, 59%, 60%, 63% and 46% for *Puccinia triticina*, *Puccinia graminis* f. sp. *tritici*, *Fusarium graminearum*, *C. neoformans*, *N. crassa*, *M. oryzae* and *S. cerevisiae*, respectively. PstSTE12 shows highest similarity to STE12 orthologues

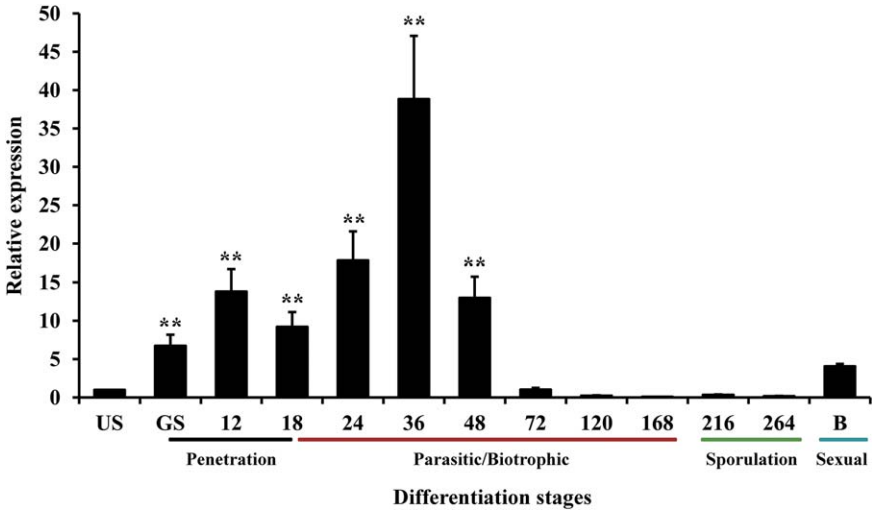

Fig. 1 Quantitative reverse transcription-polymerase chain reaction (RT-PCR) assay of transcript profiles of *PstSTE12* during *Puccinia striiformis* f. sp. *tritici* (*Pst*) infection stages. The relative transcript levels of *PstSTE12* were calculated by the comparative *Ct* method compared with an endogenous standard *elongation factor-1* (*EF-1*) gene. *Pst* infection of wheat can be divided into three major stages: 'penetration' (black), 'parasitic/biotrophic' (red) and 'sporulation' (green). Pycniospores in the alternative host berberis (*Berberis shensiana*) are marked in blue. US, urediniospores; GS, germinated urediniospores; 12–264 h, 12–264 h post-inoculation with CYR32; B, infected *Berberis shensiana*. Data represent the mean of three biological replicates ± standard error (SE). Differences were assessed using Student's *t*-test. Double asterisks indicate $P < 0.01$.

from *P. graminis* f. sp. *tritici* and *P. triticina*, and three proteins show high conservation with other STE12 proteins in the HDs.

STE12 proteins from different pathogens were selected to study their relationships. The maximum-likelihood (ML) phylogenetic analysis of PstSTE12 with orthologues from other fungi revealed that PstSTE12 displays higher similarity to STE12-like proteins from basidiomycetes, compared with those from ascomycetes (Fig. S1B). The filamentous ascomycetes containing a C_2H_2 domain were clustered into one clade, whereas yeasts without this domain were clustered into another clade (Fig. S1B). BLAST analysis showed two C_2/H_2-Zn^{2+} finger domains in the C-terminus of PstSTE12 (Fig. S2, see Supporting Information).

PstSTE12 is highly induced in *Pst* during early infection stages in wheat and in pycniospores in barberry

To address the role of *PstSTE12* during the infection stages of *Pst* with Su11, we compared the abundance of *PstSTE12* in urediniospores, germ tubes, parasitic invasion hyphae, sporulation and pycniospores in barberry (*Berberis shensiana*) (Fig. 1). Values are expressed relative to an endogenous *Pst* reference *elongation factor-1* (*EF-1*) gene, with the *PstSTE12* transcripts in ungerminated urediniospores set to unity as the control (Cheng *et al.*, 2015). The results showed that, once CYR32 contacted the leaf surface of Su11, the expression of *PstSTE12* transcripts increased and gradually reached a maximum: an approximately 40-fold increase at 36 h post-inoculation (hpi) compared with that in the control. This occurred in the initial 'parasitic/biotrophic' stage during successful expansion of *Pst* into wheat. The transcript levels of *PstSTE12* in the late 'parasitic/biotrophic' stage at 72–168 hpi and the 'sporulation' stage were down-regulated compared with that of ungerminated urediniospores. In addition, the expression of *PstSTE12* was induced four-fold compared with the control during the pycniospore stage in the aecial host barberry [11 days post-inoculation (dpi)] (Fig. 1), which is an alternative host for *Pst* (Jin *et al.*, 2010; Zhao *et al.*, 2016). The results suggest that, in addition to a role in sexual reproduction, *PstSTE12* also participates in virulence.

PstSTE12 shows transcriptional activation in yeast

To examine the transcriptional activity of *PstSTE12*, the fusion plasmids pBD-*PstSTE12*$_{1–879}$, pBD-*PstSTE12*$_{1–400}$ and the negative control pGBKT7 were separately transformed into yeast strain AH109 (Fig. 2). On selective dropout/–tryptophan (SD/–Trp) medium, clones of the three vectors transformed separately grew well, indicating the success of merging with the yeast strain (Fig. 2B). In contrast, only yeast cells containing the pBD-*PstSTE12*$_{1–879}$ vector grew on the selective dropout/–tryptophan–histidine–adenine (SD/–Trp–His–Ade) medium (Fig. 2C), whereas yeast cells with the pBD-*PstSTE12*$_{1–400}$ or negative control pGBKT7 vector did not survive. In the assay for the evaluation of α-galactosidase activity, transformants containing the pBD-*PstSTE12*$_{1–879}$ vector turned blue on SD/–Trp–His–Ade medium containing 5-bromo-4-chloro-3-indolyl α-D-galactopyranoside (X-α-Gal) (Fig. 2C), suggesting that *PstSTE12* effectively activated the transcription of

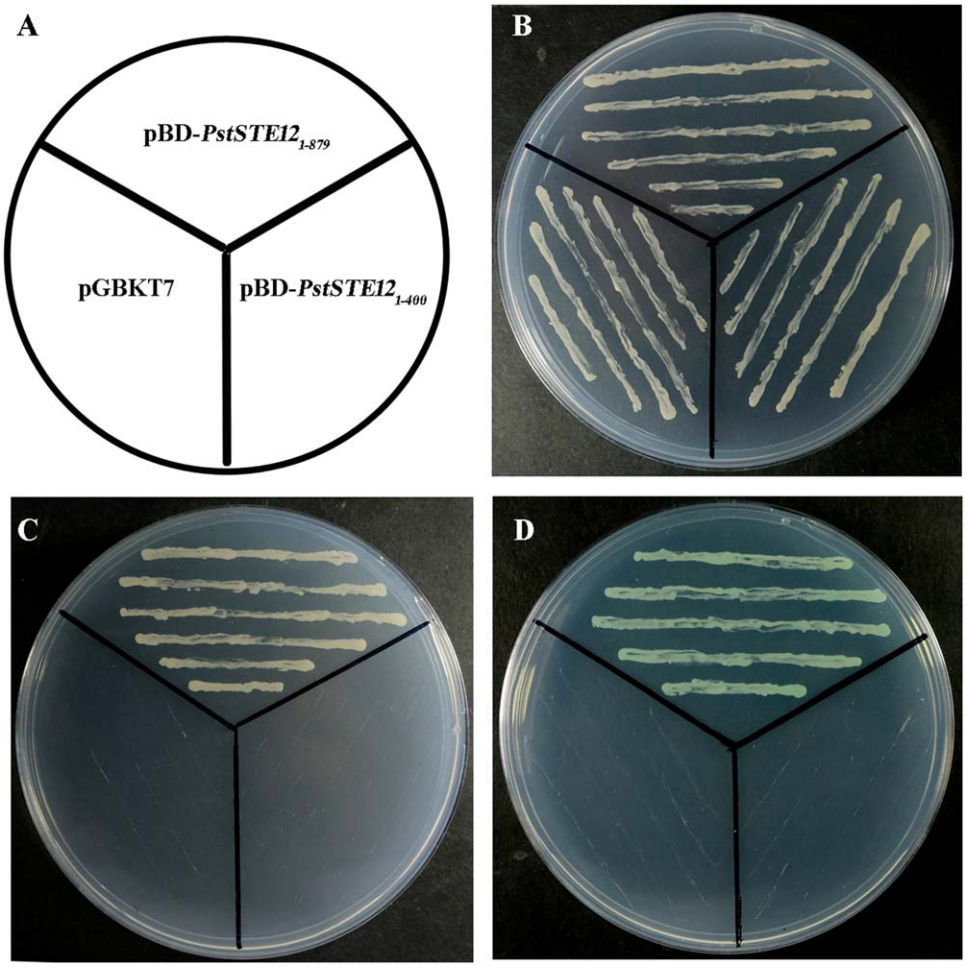

Fig. 2 Transactivation analysis of the PstSTE12 protein in yeast. The fusion and control vectors were separately transformed into the yeast strain AH109. (A) The diagram indicates the corresponding vector for the assay. (B) The transformants were selected by growth on selective dropout/–tryptophan (SD/–Trp) medium at 30 °C for 3 days. (C) Transformants were streaked onto selective dropout/–tryptophan–histidine–adenine (SD/–Trp–His–Ade) medium. (D) The α-galactosidase assay was conducted on SD/–Trp–His–Ade medium containing 5-bromo-4-chloro-3-indolyl α-D-galactopyranoside (X-α-Gal).

His3 together with *LacZ* reporter genes. However, the C-terminal deletion mutant of *PstSTE12* lost the ability to activate the transcription of the reporter genes.

PstSTE12 localizes to the nucleus of plant cells

To determine the subcellular localization of PstSTE12, we generated the fusion constructs pCaMV35S:*PstSTE12-GFP* and pCAMBIA-1302:*PstSTE12-GFP*, which were transformed into *Triticum aestivum* protoplasts with polyethyleneglycol (PEG)-calcium (Fig. 3A) or into *Nicotiana benthamiana* leaf cells by infiltration into *Agrobacterium tumefaciens* (Fig. 3B), respectively. When a PstSTE12-green fluorescent protein (GFP) fusion protein was transiently expressed in *T. aestivum* protoplasts with the pCaMV35S:*PstSTE12-GFP* construct, fluorescence was restricted to the nucleus, whereas GFP was distributed in the cytoplasm, cytomembrane and the nucleus of protoplasts in controls (Fig. 3A). When we transiently expressed the PstSTE12-GFP fusion protein in *N. benthamiana* leaf cells, we found that the GFP fusion protein again only localized to the nucleus (Fig. 3B), whereas GFP was expressed throughout the cells in controls. These data indicate that *PstSTE12* is constitutively expressed and localized to the nucleus.

Complementation of the *S. cerevisiae ste12* (α) mutant with *PstSTE12* restores mating efficiency

To verify whether *PstSTE12* might possess a function similar to the yeast *STE12* gene, we introduced *PstSTE12* into a *ste12* (α) mutant to test for complementation and a mutant rescue phenotype (Fig. S3, see Supporting Information). For the *STE12* reporter, the mating efficiency was drastically reduced to approximately 0% in the *ste12* mutants, whereas the mating efficiency in the wild-type was 100% (Fig. 4A,B) (Hartwell, 1980; Yuan *et al.*, 1993). Mating was assessed by quantitative assays. In accord with previous studies, our data showed that mating of the empty vector transformants occurred at an extremely low frequency (nearly 0%), consistent with the mutant type (Fig. 4). Meanwhile, the complemented strain, formed when the *PstSTE12* gene was introduced into the *ste12* mutant, mated with the wild-type *MATa*, led to a recovery of 34% mated cells. Percentage data were calculated by dividing the mating efficiency of each construct by the mating

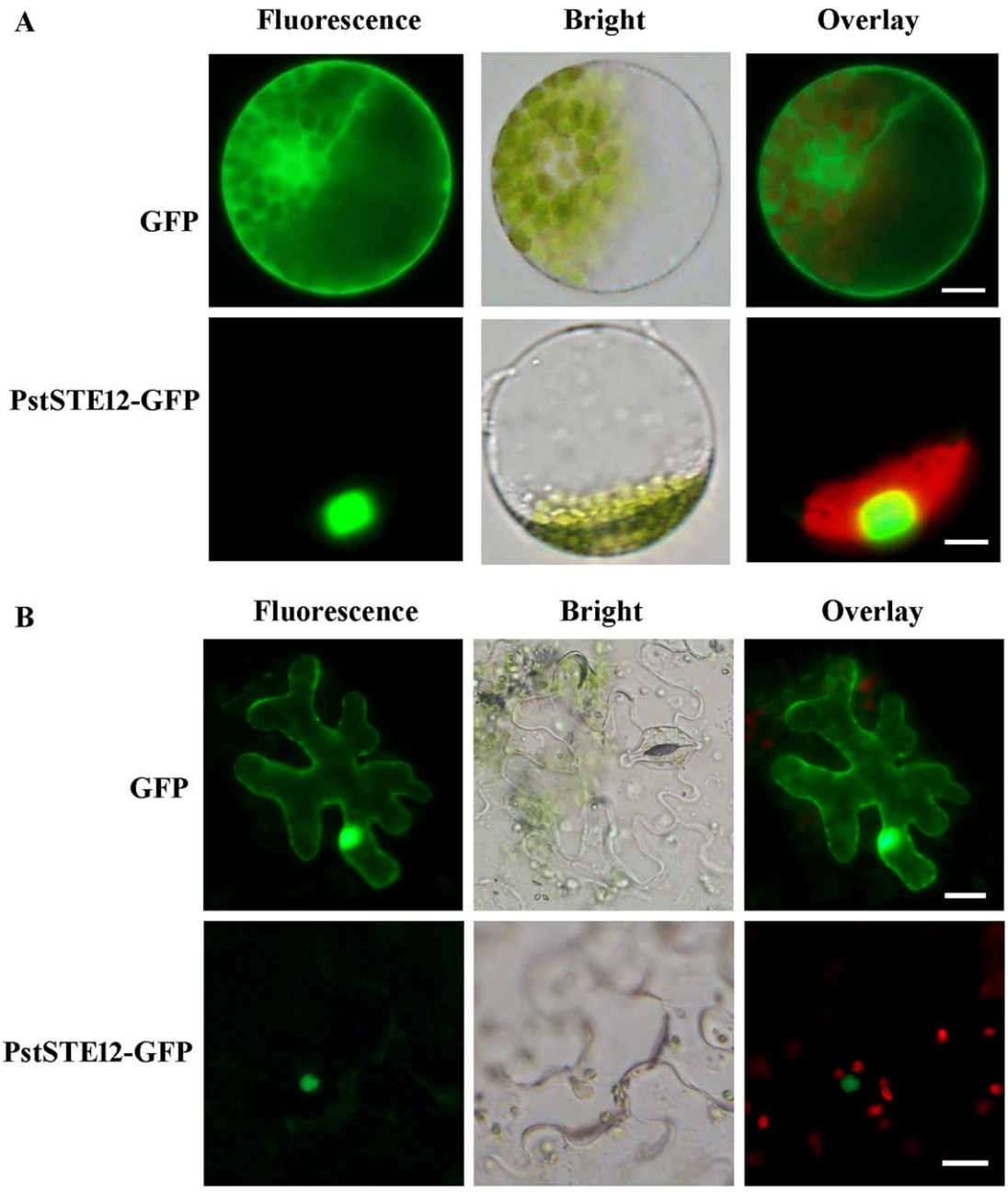

Fig. 3 Subcellular localization of the PstSTE12 protein. All images were observed using a fluorescence microscope. (A) Green fluorescent protein (GFP) (control) and *PstSTE12*-GFP fusion protein were expressed in wheat protoplasts following polyethyleneglycol (PEG)-mediated transformation. Bar, 10 μm. (B) GFP and PstSTE12-GFP fusion protein were expressed in *Nicotiana benthamiana* by transient agro-infiltration assays. Bar, 20 μm. The fluorescence channel shows the localization of GFP and PstSTE12-GFP (green). The bright channel shows the integrity of cells or protoplasts. An overlay of micrographs shows GFP and PstSTE12-GFP (green) together with the chloroplasts (red).

efficiency of the wild-type. Then, the ascospores were germinated in MacConkey medium and yeast cells were stained with phenol and methylene blue after growth for 5–6 days. Microscopic examination revealed blue conidia and red ascospores. The results indicated that both the yeast mutant *ste12* (α) and the mutant carrying the empty vector failed to mate with *MATa* wild-type cells (Fig. 4C). However, the wild-type strains of yeast *a*/α and transformants of *ste12*/*PstSTE12*(α) mating with *MATa* wild-type cells produced not only conidia, but also ascospores (Fig. 4C), confirming the successful mating with *MATa*. These results show that *PstSTE12* can partially complement the *ste12* mutation and suggest that it may be involved in the mating pathway in *Pst*.

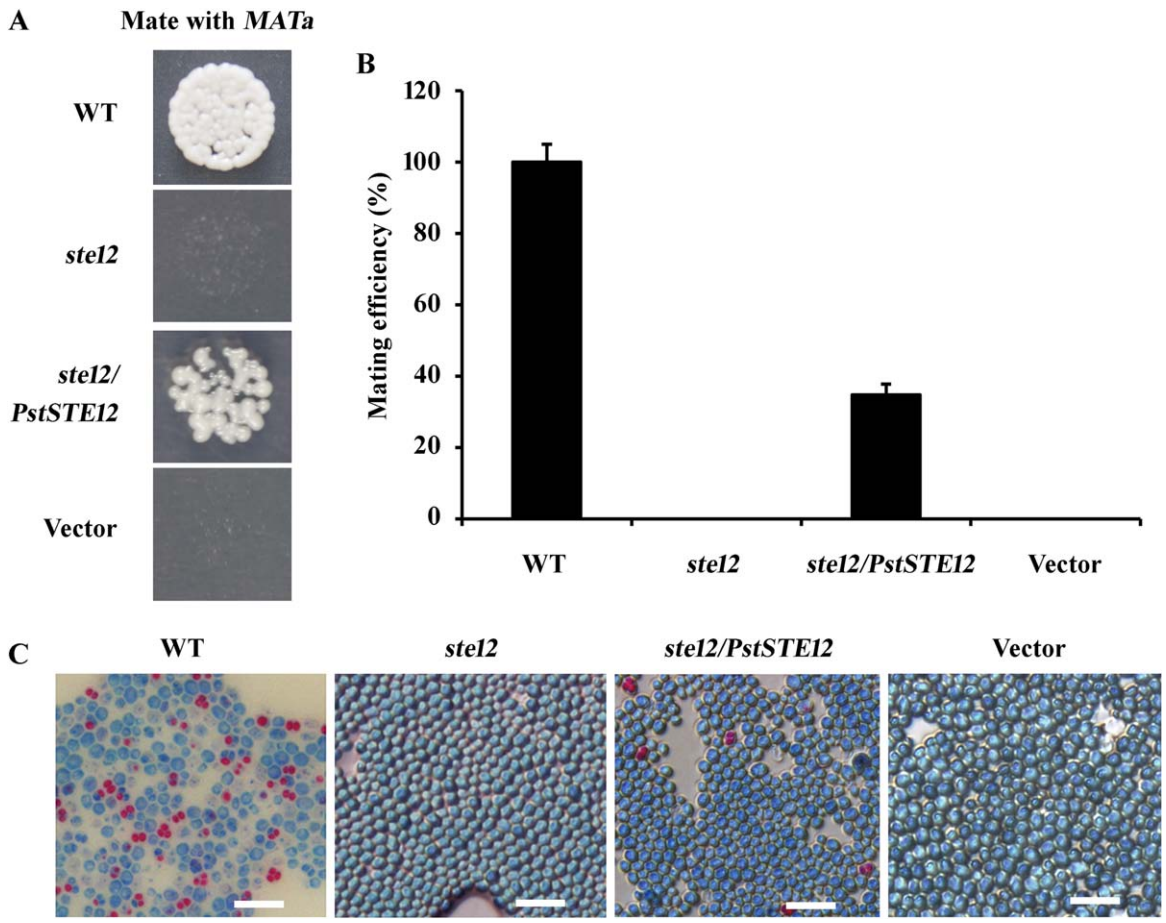

Fig. 4 Functional characterization of the *PstSTE12* transcription factor in the *Saccharomyces cerevisiae ste12* mutant. (A) Patch mating assays for the ability of the wild-type, mutant and transformant strains mated with the wild-type *MATa* cells. *PstSTE12* and empty vector were transformed into *S. cerevisiae ste12* mutants. The strains were transferred onto a minimal plate spread with cells of the opposite mating type. (B) Quantitative assay of the mating efficiency. The mating efficiency of constructs was calculated as a percentage by dividing with the mating efficiency of wild-type *a*/α. (C) Conidium and ascospore are labelled with blue and red, respectively. From left to right: the wild-type strain of yeast *MATa/MAT*α; *ste12* (α) mutant mating with *MATa* wild-type cells; transformants of *ste12*/*PstSTE12* mating with *MATa* wild-type; transformants carrying the empty vector mating with *MATa* wild-type strains. Bar, 10 μm.

PstSTE12 partially complements the function of *mst12* mutants in *M. oryzae*

The TF *MST12* is required for infectious growth, but not appressorium formation, in *M. oryzae* (Park *et al.*, 2002). To test whether *PstSTE12* can functionally complement the *mst12* mutant in *M. oryzae*, we transformed the *PstSTE12* gene under the control of the strong constitutive RP27 promoter into the *mst12* mutant (Park *et al.*, 2002). Geneticin-resistant transformants were isolated and verified by PCR to confirm the introduction of *PstSTE12*. Mature appressoria formed by the *mst12* mutant were normal in size with typical morphology and melanization. Thus, appressorium formation was not significantly different between the transformants and wild-type (Park *et al.*, 2002; Zhou *et al.*, 2011) (Fig. 5A). However, unlike appressoria formation, the *mst12* mutant was defective in infection of barley and rice (Zhou *et al.*, 2011). To determine whether *PstSTE12* could recover the virulence of the *mst12* mutant, 8-day-old barley seedlings of cultivar NB6 were drop inoculated with conidia. At 6 dpi, leaves inoculated with the wild-type developed typical blast lesions (Fig. 5B). No lesions were observed on leaves inoculated with gelatin and the *mst12* mutant also failed to cause lesions on barley leaves (Fig. 5B). Under the same conditions, transformants caused obvious lesions on barley leaves. These results indicate that *PstSTE12* can partially complement the function of *mst12* in plant infection.

Silencing of *PstSTE12* reduces virulence of *Pst* on wheat

To further characterize the function of *PstSTE12* during the interaction between wheat and *Pst*, *Barley stripe mosaic virus* (BSMV) virus-induced gene silencing (VIGS) was used in this study (Cheng *et al.*, 2015; Yin *et al.*, 2011). Two different ~250-bp fragments (BSMV:*PstSTE12*-H and BSMV:*PstSTE12*-B) were designed to

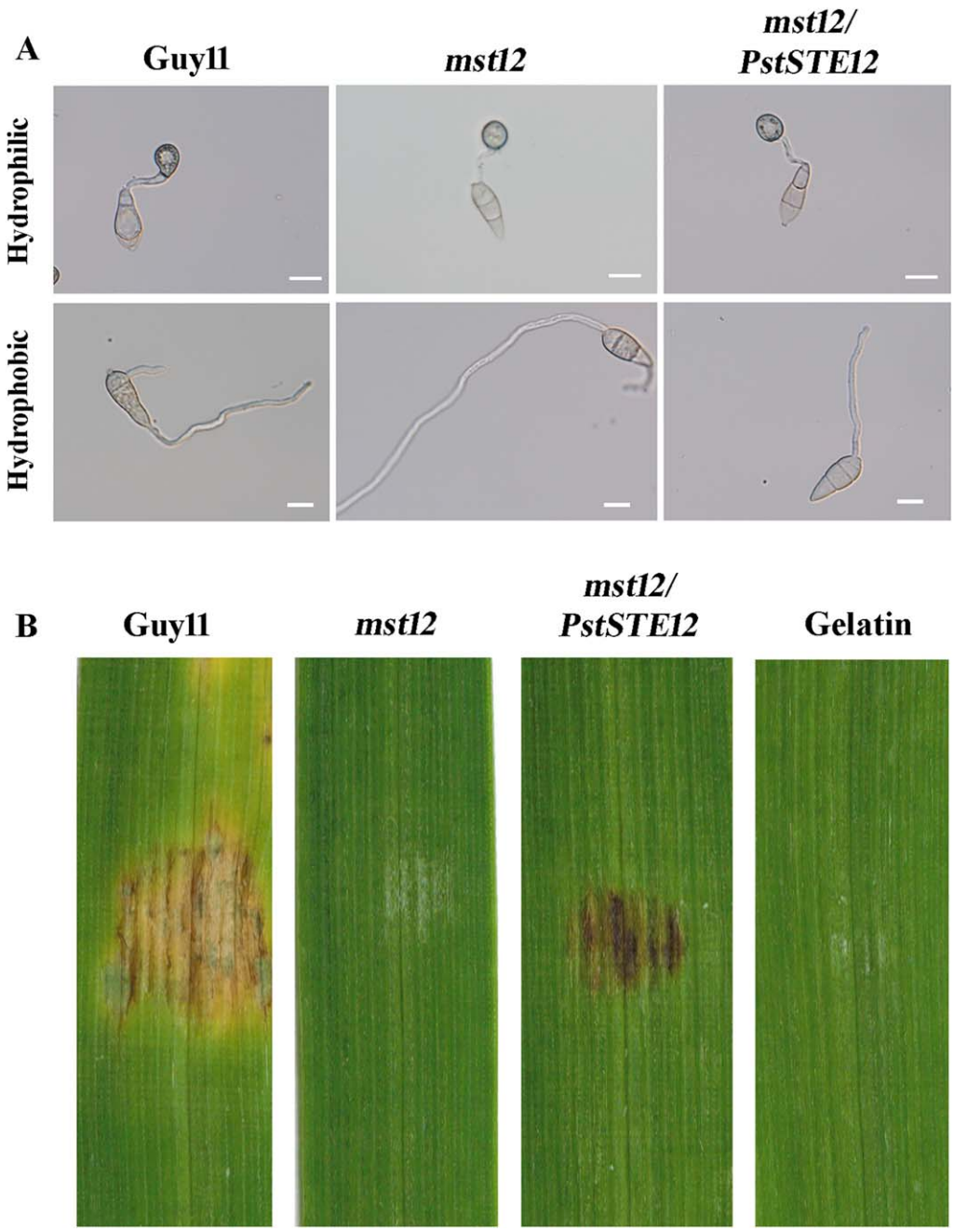

Fig. 5 Complementation of the *mst12* mutant with the pFL2-*PstSTE12* fusion construct. (A) Appressorium formation assays on hydrophobic and hydrophilic surfaces. Appressoria were formed by the wild-type Guy11 and the *mst12* mutant transformants on the hydrophobic (bottom) and hydrophilic (top) surfaces of Gelbond membranes at 24 h. Bar, 10 μm. (B) Barley infection assay. From left to right: barley leaves inoculated with conidia of Guy11, *mst12* mutant, transformants and 0.25% gelatin. Typical phenotypes were photographed at 6 days post-inoculation (dpi).

specifically silence *PstSTE12* (Fig. S4, Table S1, see Supporting Information). The assay was performed in wheat cv. Su11, which is susceptible to *Pst* isolate CYR32. All of the plants infected with virus, BSMV:γ, BSMV:*PstSTE12*-H or BSMV:*PstSTE12*-B, displayed mild chlorotic mosaic symptoms at 10 dpi, whereas mock-inoculated plants were green and healthy (Fig. 6A). Subsequently, the fourth leaves were inoculated with urediniospores of *Pst* CYR32 on mock- and virus-inoculated plants. After 14 days, very few uredinia were produced on leaves previously infected with BSMV:*PstSTE12*-H or BSMV:*PstSTE12*-B (Fig. 6B,C). In contrast, mock-inoculated leaves and leaves infected with BSMV:γ inoculated with CYR32

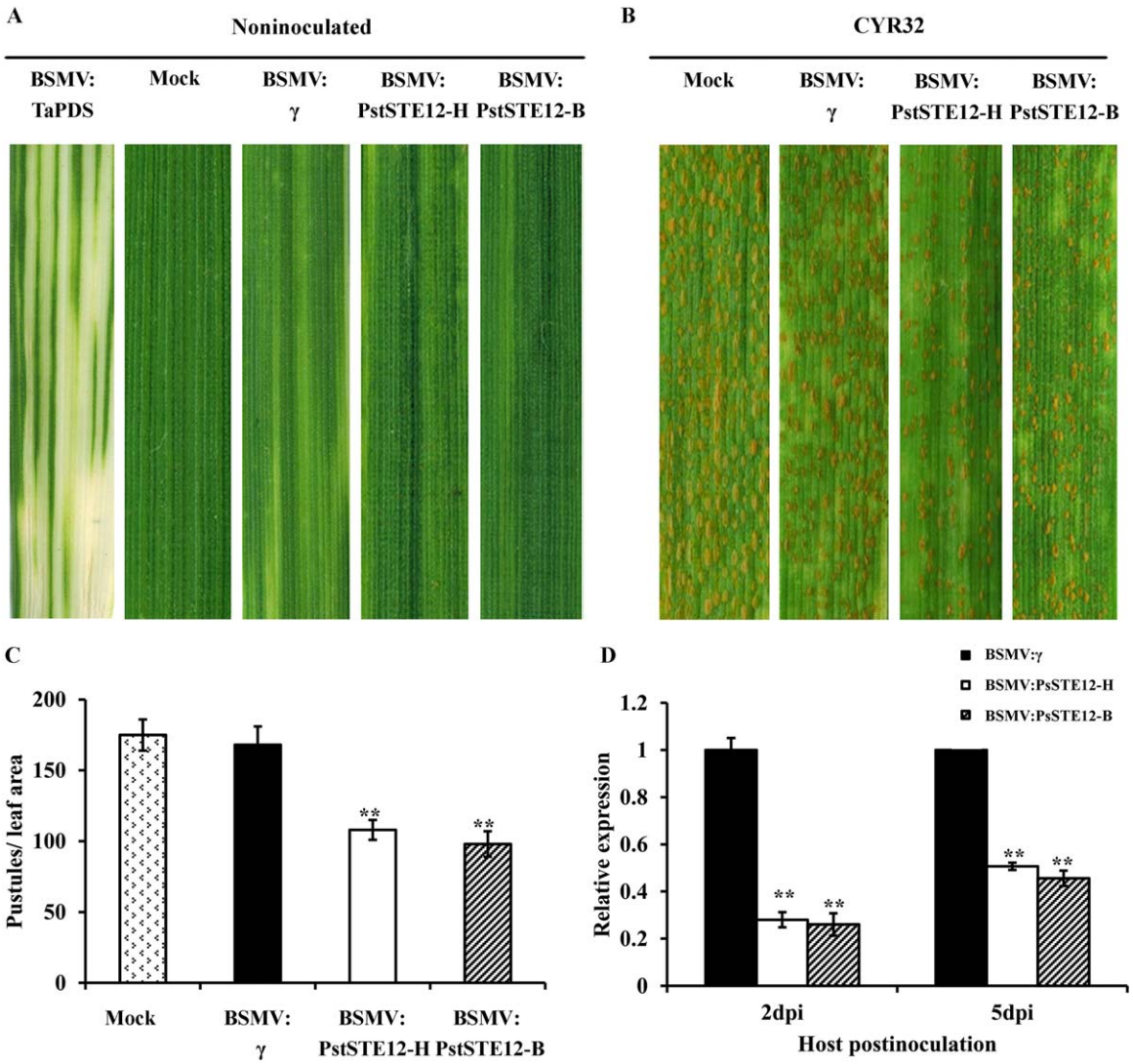

Fig. 6 Silencing of *PstSTE12* in the wheat–*Puccinia striiformis* f. sp. *tritici* (*Pst*) interaction using host-induced gene silencing (HIGS) leads to reduced virulence. (A) No change in phenotype was observed in wheat leaves mock inoculated with FES buffer. Mild chlorotic mosaic symptoms were observed in wheat leaves inoculated with BSMV:γ, BSMV:*PstSTE12*-H and BSMV:*PstSTE12*-B. Photobleaching was evident on wheat leaves infected with BSMV:*TaPDS*. (B) Phenotypes of the fourth leaves of wheat plants inoculated with mock (FES buffer), BSMV:γ, BSMV:*PstSTE12*-H and BSMV:*PstSTE12*-B at 14 days post-inoculation (dpi) with the virulent *Pst* isolate CYR32. (C) Quantification of uredinial density in silenced plants at 14 dpi with the CYR32 isolate. Values represent mean ± standard errors of three independent assays. Differences were assessed using Student's *t*-tests. Double asterisks indicate $P < 0.01$. (D) Relative levels of *PstSTE12* transcript abundance in knock-down wheat leaves. RNA samples were isolated from the fourth leaves of wheat infected with BSMV:γ, BSMV:*PstSTE12*-H and BSMV:*PstSTE12*-B at 48 and 120 h post-inoculation (hpi) with the CYR32 isolate. Values are expressed relative to an endogenous *Pst* reference *elongation factor-1* (*EF-1*) gene, with the empty vector (BSMV:γ) set at unity. Values represent mean ± standard errors (error bars) of three independent samples. Differences were assessed using Student's *t*-tests. Double asterisks indicate $P < 0.01$.

produced numerous uredinia with abundant urediniospores (Fig. 6B,C). To determine the efficiency of knockdown by HIGS, transcript levels of *PstSTE12* were detected at 48 and 120 hpi with the CY32 isolate. Compared with transcription levels of *PstSTE12* in leaves inoculated with BSMV:γ, the expression of *PstSTE12* was knocked down by 72% and 49% in leaves inoculated with BSMV:*PstSTE12*-H at 48 and 120 hpi with the CYR32 isolate, respectively (Fig. 6D). Similarly, in leaves inoculated with BSMV:*PstSTE12*-B, transcripts of *PstSTE12* were reduced by 74% and 54% at 48 and 120 hpi with the CYR32 isolate, respectively (Fig. 6D). These findings indicate that, overall, the level of transcription of *PstSTE12* is reduced in the invading fungus, and that this silencing probably influences the expression of *PstSTE12* in *Pst*.

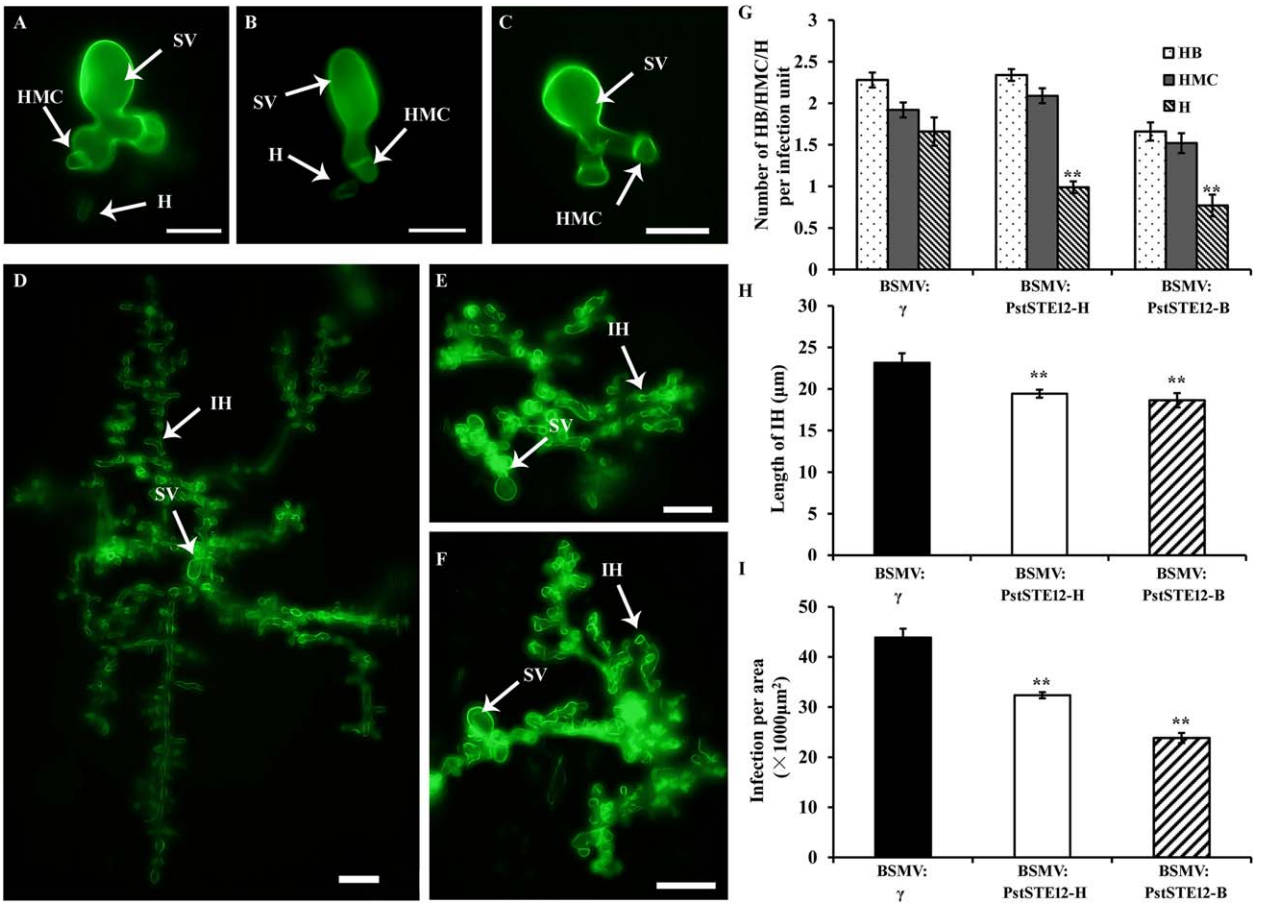

Fig. 7 Histological observation of fungal growth in wheat infected with BSMV:γ and recombinant *Barley stripe mosaic virus* (BSMV) after inoculation with CYR32. (A–C) Fungal growth at 24 h post-inoculation (hpi) in BSMV:γ-infected plants (A), BSMV:*PstSTE12*-infected plants (B) and BSMV:*PstSTE12*-B-infected plants (C). Bar, 20 μm. (D–F) Fungal growth at 120 hpi in BSMV:γ-infected plants (D), BSMV:*PstSTE12*-H-infected plants (E) and BSMV:*PstSTE12*-B-infected plants (F). Bar, 50 μm. (G) The numbers of branches of infection hyphae (HB), haustorial mother cells (HMC) and haustoria (H) per infection unit were recorded at 48 hpi. (H) The length of infection hyphae (IH) in *PstSTE12*-silenced plants at 48 hpi with the CYR32 isolate. The length of IH was measured from the substomatal vesicle to the apex of the longest infection hypha. (I) The infection unit area per infection unit was determined at 120 hpi. Values represent the means ± standard errors of three independent samples. Differences were assessed using Student's *t*-tests. Asterisks indicate $P < 0.05$. Double asterisks indicate $P < 0.01$. SV, substomatal vesicle.

HIGS of *PstSTE12* compromises fungal growth in the interaction between *Pst* and wheat

To determine how *PstSTE12* is involved in *Pst* pathogenicity, we observed the cytological changes in *PstSTE12*-silenced plants inoculated with *Pst* CYR32 at 48 hpi (Fig. 7A–C) and 120 hpi (Fig. 7D–F). The number of haustorial mother cells, as well as the number of hyphal branches, hyphal length and hyphal areas, were counted, as indicators of fungal penetration and expansion abilities, respectively (Fu *et al.*, 2014; Tang *et al.*, 2015). The numbers of haustorial mother cells and hyphal branches were not significantly different from controls at 48 hpi (Fig. 7G). However, the numbers of haustoria were significantly reduced in *PstSTE12*-silenced plants (Fig. 7G). Moreover, hyphal lengths in *PstSTE12*-silenced plants were shorter than those observed in BSMV-γ-treated leaves at 48 h ($P < 0.01$) (Fig. 7H). Consistent with this, hyphal expansion areas of *Pst* were strictly limited in *PstSTE12*-silenced plants at 120 hpi. In contrast, control plants treated with BSMV:γ showed extensive colonization and the formation of secondary hyphae (Fig. 7D–F,I). These results indicate that *PstSTE12* most probably contributes to fungal growth by participating in haustorium formation and hyphal development. Thus, *PstSTE12* may also be involved in the invasion and pathogenicity of *Pst*.

DISCUSSION

The frequency of variation in cereal rust fungi often results in a rapid and sudden loss of resistance to *Pst* in cultivated wheat. Sexual reproduction is the primary process contributing to the origin of new races with combined virulence genes and diversification of stripe rust pathogens (Zhao *et al.*, 2016). Although some virulence-related genes have been described in *Pst* (Cheng *et al.*,

2015; Liu *et al.*, 2016; Tang *et al.*, 2015), fewer studies have documented the genes that are involved in mating in *Pst*. A previous study has reported that the orthologue *STE12*, together with other components, contributes to the regulation of fertility in sexual crosses in heterothallic fungi, such as *S. cerevisiae* (Fields and Herskowitz, 1985; Hartwell, 1980; Rispail and Pietro, 2010). In this study, we identified and characterized *PstSTE12*, which shares structural features with STE12 orthologues in other fungi (Hoi and Dumas, 2010; Rispail and Pietro, 2010). The structural conservation of MAP kinase cascades between *Pst* and other fungal pathogens suggests a possible role of *STE12* as a downstream target in different signalling pathways. In support of this hypothesis, we found that the expression of *PstSTE12* restored the fertility in a *ste12* mutant. Given the functional conservation properties of genes between different species, the recovery of the mating efficiency of the *ste12* mutant complemented with *PstSTE12* suggests that the function of PstSTE12 is conserved with yeast STE12. Possibly, *PstSTE12* plays an important role in the mating pathway in *Pst*. *Ustilago maydis* is the most advanced model plant pathogen in basidiomycetes and lacks a STE12 orthologue (Brefort *et al.*, 2005). A STE12 orthologue has been well characterized in the human pathogen model basidiomycete *C. neoformans*. In *C. neoformans*, *CnSTE12α* and *CnSTE12a* are required for haploid fruiting, and deletion of *CnSTE12α* or *CnSTE12a* reduces the mating frequency and virulence in mice (Chang *et al.*, 2000, 2001). In this regard, it is of interest to note that we found that *PstSTE12* was clearly expressed during the pycniospore stage in the aecial host barberry, a crucial stage of the reproduction process. The role of sexual reproduction in generating variation in virulence in *Pst* was not confirmed until the alternative host *Berberis* was discovered (Jin *et al.*, 2010; Wang and Chen, 2013; Zhao *et al.*, 2013). On alternative hosts, receptive hyphae are fertilized by pycniospores from other pycnia of the compatible mating type to produce dikaryotic mycelia, and then produce aecia containing one-celled aeciospores with two nuclei (n + n) (Zhao *et al.*, 2016). Thus, *PstSTE12* may take part in the mating pathway by keeping the nuclei in communication during the dikaryotic stage, and contribute to virulence variation by generating new races through sexual reproduction.

The *STE12* gene in *S. cerevisiae* encodes a protein that binds to the pheromone-responsive element sequence in the nucleus, which is present in many different a- and α-specific upstream regulatory sequences (Blackwell *et al.*, 2007). As a TF, the PstSTE12 protein was predicted to contain a nuclear localization signal, and we confirmed that PstSTE12 was localized to the nucleus in heterologous (plant) systems. Cell surface receptors respond to the extracellular stimuli that induce a cascade of transduction signals, resulting in phosphorylation of various proteins positioned downstream in a variety of pathways, including the STE12 protein (Hamel and Ellis, 2012; Meng and Zhang, 2013; Rispail and Pietro, 2010). This rapid phosphorylation is associated with an increase in the ability of *STE12* to stimulate transcription in the nucleus. We inferred that *PstSTE12* may perform similar functions in *Pst*. The yeast one-hybrid assay further showed that PstSTE12 has transcriptional activity and that the C-terminal region (400–879 amino acids) is necessary for transactivation. Similarly, in *S. cerevisiae*, the removal of large C-terminal regions of *STE12* significantly reduced basal transcription. This cooperativity of *STE12* to bind a single pheromone response element, such as that present in the *STE2* gene, together with the binding of MCM1 to an adjacent site, requires the carboxyl-terminal domain of STE12 (Kirkman-Correia *et al.*, 1993). These data suggest that *PstSTE12* is a *Pst* TF, which may function as a transcriptional activator in the fungal nucleus.

STE12 positioned downstream of the MAP kinase pathway in *S. cerevisiae* also participates in filamentous invasive growth (Madhani and Fink, 1997; Rispail and Pietro, 2010). In addition, various orthologous STE12-like proteins of pathogenic fungi, such as in *M. oryzae*, have been reported to regulate infection processes (Park *et al.*, 2002; Zhou *et al.*, 2011) and *F. graminearum* (Yang *et al.*, 2015). In *M. oryzae*, germination and appressorium formation of the *mst12* mutant were normal, but, in infection assays, the *mst12* mutants appeared to be non-pathogenic (Park *et al.*, 2002). Our study showed that the expression of the *PstSTE12* gene can partially restore function in the *M. oryzae mst12* mutant. The *PstSTE12*-transformed mutants showed restored function in appressorium penetration and invasive growth, suggesting that *PstSTE12* plays a potential role in virulence in *Pst*. However, the phenotypes of the *PstSTE12*-transformed mutants could not be entirely rescued, indicating that *PstSTE12* is not fully functional in this ascomycete fungus, and also that there is specificity between different fungi. *Pst*, as an obligate parasitic pathogen, has a special and complex life style (Zheng *et al.*, 2013), which is substantially different from that of *M. oryzae*. During evolution, sequence and structural variation in *PstSTE12* may have enabled it to distinguish various environmental stimuli. This may reduce the functional efficiency of *PstSTE12* in signal transduction in ascomycetes and account for the partial recovery of the phenotype. We also showed by quantitative reverse transcription-polymerase chain reaction (qRT-PCR) that the *PstSTE12* gene is highly induced during *Pst* infection and functions as an important pathogenicity factor. *PstSTE12* was clearly expressed during fungal colonization, haustorium formation, primary hyphal extension and sexual reproduction. A role in virulence was supported by further evidence via observations in HIGS experiments. Just as deletion of *STE12* leads to defects in penetration and invasive growth in other fungi (Rispail and Di, 2009; Tsuji *et al.*, 2003), silencing of *PstSTE12* strongly reduces *Pst* virulence (Fig. 7). Silencing of *PstSTE12* restricts

Pst haustorium formation and development at 48 hpi, whereas the extension area of secondary hyphae and fungal colonization are significantly reduced at 120 hpi with the CYR32 isolate, suggesting that silencing of *PstSTE12* at the early stages of infection suppresses further development at later stages. The growth of *Pst* was significantly limited, as indicated by the generation of a reduced number of uredinia on wheat leaves after 14 days. Our data suggest that *PstSTE12* plays an important role in plant infection by regulating haustorium formation and fungal colonization. Collectively, our results, together with previous studies, provide strong circumstantial evidence suggesting that *PstSTE12* plays a key role in the regulation of the response of infection signals lying downstream of a signal pathway network in *Pst*, and may be involved in the mating process. Therefore, future identification and characterization of rust fungi-specific targets of *PstSTE12* should result in a more complete understanding of the evolution of pathogenesis and virulence in *Pst*.

EXPERIMENTAL PROCEDURES

Plant materials, strains and treatments

The wheat (*T. aestivum*) cultivar Suwon11 (Su11), which is highly susceptible to *Pst* isolate CYR32, was used in this study. Wheat was cultivated and inoculated by the procedures and conditions described previously (Kang *et al.*, 2002). To investigate the *PstSTE12* transcript profiles, samples were collected at 12, 18, 24, 36, 48, 72, 120, 168, 216 and 264 hpi during the CYR32 interaction with Su11, and in barberry (*Berberis shensiana*) leaves inoculated with CYR32 basidiospores at 11 dpi, which is the pycniospore stage in the aecial host barberry. After incubation at 4 °C for 6 h, germinated urediniospores were collected and frozen in liquid nitrogen for RNA extraction. The developmental stages of the *Pst* infection process analysed by qRT-PCR were the same as those described previously (Cheng *et al.*, 2015). Disease symptoms were photographed at 15 dpi. Three independent biological replicates were performed for each treatment.

RNA isolation and qRT-PCR analysis

Total RNA was isolated using RNAiso Reagent (TaKaRa, Tokyo, Japan) according to the manufacturer's instructions. First-strand cDNA was synthesized using the RevertAid First Strand cDNA Synthesis Kit (Thermo Scientific, Waltham, MA, USA) with an oligo(dT)18 primer as instructed. qRT-PCR was performed on a CFX Connect Real-Time System (Bio-Rad, Hercules, CA, USA). EF-1 was used as internal control to normalize the gene expression in *Pst* (Liu *et al.*, 2016). Reactions were performed on a 7500 Real-Time PCR System (Applied Biosystems, Foster City, CA, USA) under the conditions described by Cheng *et al.* (2015). The relative transcript expression was assessed by the $2^{-\Delta\Delta Ct}$ method with three biological replicates (Livak and Schmittgen, 2001).

Isolation, cloning and sequence analysis of *PstSTE12*

PCR amplification of the *PstSTE12* gene was performed using a CYR32-inoculated Su11 cDNA sample as a template. The PCR products were purified and cloned into the pGEM-T vector (Promega, Madison, Wisconsin, USA) and sequenced. Target P (http://www.cbs.dtu.dk/services/TargetP/) was used to predict the subcellular localization of *PstSTE12*. Multiple sequence alignments between homologous proteins from other fungi were compared using CLUSTALW (version 1.8) software and added shade by Boxshade online (http://www.ch.embnet.org/software/BOX_form.html). MEGA5 was used for phylogenetic analysis by the ML method. Some of the STE12 orthologues were obtained from the National Center for Biotechnology Information (NCBI) (https://www.ncbi.nlm.nih.gov/), including *Aspergillus nidulans* (XP_659894.1), *Aspergillus oryzae* (KDE77588.1), *Talaromyces marneffei* (ABH09729.1), *Setosphaeria turcica* (AFS49719.1), *Marssonina brunnea* (EKD19163.1), *Botrytis cinerea* (ACJ06644.1), *Sclerotinia borealis* (ESZ98034.1), *Colletotrichum lagenaria* (BAC11803.1), *C. lindemuthianum* (CAD30840.2), *Cryphonectria parasitica* (ABE67104.1), *M. oryzae* (AAL27626.2), *Trichoderma reesei* (EGR50918.1), *F. graminearum* (XP_387486.1), *Fusarium oxysporum* (ACM80357.1), *N. crassa* (AAK14814.1), *S. cerevisiae* (KZV10819.1), *Kluyveromyces lactis* (AAA35270.1), *P. triticina* (PTTG_05606T0), *P. graminis* f. sp. *tritici* (EFP80971.2), *Peronosclerospora sorghi* (KNZ61697.1), *Melampsora larici-populina* (EGF98701.1), *Mixia osmundae* (XP_014567023.1), *Trichosporon asahii* (EKC98332.1), *Xanthophyllomyces dendrorhous* (CED85281.1), *Cryptococcus gattii* (AAS92520.1), *C. neoformans* (AAN75715.1), *Candida albicans* (AAA64692.1) and *Clavispora lusitaniae* (AAD51741.1). The others were obtained from Ensembl Fungi (http://fungi.ensembl.org/index.html), including *Trichosporon oleaginosus* (KLT46070), *Pisolithus microcarpus* (KIK17142), *Scleroderma citrinum* (KIM53342), *Hypholoma sublateritium* (KJA26649), *Laccaria amethystina* (KIJ98362) and *Laccaria bicolor* (EDR03059).

Subcellular localization analysis

A pCAMBIA1302:*PstSTE12-GFP* fusion was transformed into the *A. tumefaciens* strain GV3101 by electroporation. Individual colonies surviving after selection with kanamycin (50 μg/mL), rifampicin (30 μg/mL) and chloramphenicol (30 μg/mL) were verified by PCR with vector primers. The procedure for the infiltration of leaves was the same as that described previously (Cheng *et al.*, 2015). Infiltrated plants were grown at 25 °C with a cycle of 16 h light and 8 h darkness. Tissue samples were collected after infiltration for 2 or 3 days and observed under an Olympus BX-51 microscope (Olympus Corporation, Tokyo, Japan).

Triticum aestivum Su11 plants for protoplast transformation were grown in the glasshouse for 2–3 weeks. The plasmid pCaMV35S:*PstSTE12*-GFP and the control plasmid pCaMV35S:GFP were separately transformed into *T. aestivum* protoplasts through PEG-calcium transfection (Ito and Shinozaki, 2002; Li *et al.*, 2015). After culture for 18–24 h, the GFP signals in transformed protoplasts were observed with a fluorescence microscope (Olympus BX-51). All experiments were repeated three times, with each assay performed on at least three plants.

Transcriptional activation analysis in yeast

According to the manufacturer's instructions (Clontech, Tokyo, Japan), the reporter plasmids pBD-*PstSTE12*$_{1–879}$ and pBD-*PstSTE12*$_{1–400}$ and the negative control plasmid pGBKT7 were transformed into the yeast strain AH109 (Clontech), individually. The transformed yeast strains were cultured on SD/–Trp and SD/–Trp–His–Ade media at 30 °C, and subsequently photographed after 3 days. The α-galactosidase activity assay was evaluated with X-α-Gal as a substrate according to the manufacturer's instructions.

Complementation of *S. cerevisiae ste12* (α) mutants with *PstSTE12*

The yeast *S. cerevisiae* diploid mutant strains *ste12* (BY4743; *MATa*/*MATα*; *ura3Δ0*/*ura3Δ0*; *leu2Δ0*/*leu2Δ0*; *his3Δ1*/*his3Δ1*; *met15Δ0*/*MET15*; *LYS2*/*lys2Δ0*; *YHR084w*/*YHR084w*::*kanMX4*) and wild-type BY4741 (*MATa*; *his3D1*; *leu2D0*; *met15D0*; *ura3D0*) and BY4742 (*MATα*; *his3D1*; *leu2D0*; *lys2D0*; *ura3D0*) were purchased from the (EUROSCARF collection, Frankfurt, Germany). Tetrads of spores were arrested after plating on MacConkey medium at 30 °C for 5–7 days. The haploid mutant spores were identified as *ste12* (*MATα*; *ura3Δ0*; *leu2Δ0*; *his3Δ1*; *MET15*; *lys2Δ0*; *YHR084w*::*kanMX4*) (data not shown), and separated haploid spores were transformed with pDR195-*PstSTE12* vectors by a lithium acetate method, as directed in the user's manual (Clontech). Quantitative mating assays were performed as described previously (Passmore *et al.*, 1989; Sprague, 1991). Briefly, cultures with 2×10^6 cells of the transformants and 10^7 cells of the appropriate tester strain were mixed. The cells were plated on 1.0% yeast extract, 2.0% peptone, 2.0% glucose, 2.0% agar (YPD) plates and allowed to grow for 24 h at 30 °C, and then replica-plated onto selective media. The number of mated cells was determined by their growth on selective media. The efficiency of mating was calculated from the number of cells that mated divided by the total number of cells of the transformants in the mating reaction. The mating efficiencies of wild-type a and α strains were normalized to 100%, and the mating efficiencies of the other strains were expressed as a percentage of those of the wild-type strains. The values are the means of two independent experiments. The staining assay of ascospores was performed on cultures grown for 5–6 days on MacConkey medium, and the cells were fixed with phenol and methylene blue by the method described previously (Lanchun *et al.*, 2003).

Complementation of mutant *mst12* by *PstSTE12* in *M. oryzae*

For construction of the complementary expression vector in *M. oryzae*, the PCR products of the *PstSTE12* gene amplified with primers STE12-CF/CR (Table S1) were co-transformed with *Xho*I-digested pFL2 vector into *S. cerevisiae* strain XK1–25 (Bruno *et al.*, 2004). The *PstSTE12* gene was under the control of the strong constitutive RP27 promoter (derived from the *M. oryzae* ribosomal protein 27 gene). Then, the pFL2-*PstSTE12* construct was transformed into protoplasts of the *M. oryzae ste12* deletion mutant. Geneticin-resistant transformants were isolated and verified by PCR with primers *PstSTE12*-CF/CR to confirm that the *PstSTE12* gene had been integrated into the *M. oryzae* genome. Appressorium formation was assayed as described previously (Zhou *et al.*, 2011). For plant infection investigation, conidia were resuspended to 10^5 conidia/mL in sterile distilled water. Eight-day-old barley seedlings of cultivar NB6 were used for infection assays (Zhou *et al.*, 2011). Lesion formation was examined at 6 dpi.

Silencing by HIGS

Two cDNA fragments derived from different sites were used to silence *PstSTE12* (Fig. S4, Table S1). Fragments contained no sequence similarity with known wheat genes by BLAST analysis of the public database from NCBI, indicating the specificity of the fragments. Capped *in vitro* transcripts were prepared from linearized plasmids containing the tripartite BSMV genome (Petty *et al.*, 1990) using the RiboMAX^{TM} Large-Scale RNA Production System-T7 and the Ribom7G Cap Analog (Promega), according to the manufacturer's instructions. The surface of the second leaf of two-leaf wheat seedlings was inoculated with BSMV transcripts by mechanical rubbing, and followed by incubation at 25 °C. BSMV:*TaPDS* (TaPDS, the wheat phytoene desaturase) was used as a positive control (Holzberg *et al.*, 2002), and plants inoculated with 1 × 77 mM glycine, 60 mM K_2HPO_4, 22 mM $Na_4P2O_7 \cdot 10H_2O$, 1% [wt/vol] bentonite, and 1% [wt/vol] celite (FES buffer) were used as a negative control (Mock). Ten days after virus inoculation, phenotypes were observed and photographed. The fourth leaves were further inoculated with CYR32 urediniospores and sampled at 48 and 120 hpi for RNA isolation and cytological observation. Phenotypes were recorded and photographed at 14 dpi with CYR32. The experiment was repeated at least three times.

Histological observations of fungal growth

Wheat leaves infected with BSMV were sampled at 48 and 120 hpi with *Pst*, and stained as described previously (Wang *et al.*, 2007). Leaf segments excised from the inoculated leaves were fixed and decolorized in ethanol–trichloromethane (3 : 1, v/v) containing 0.15% (w/v) trichloroacetic acid for 3–5 days. The specimens were cleared in saturated chloral hydrate until the leaf tissue became translucent. Wheatgerm agglutinin conjugated to Alexa-488 (Invitrogen, Carlsbad, CA, USA) was used to stain samples, as described previously (Ayliffe *et al.*, 2011; Cheng *et al.*, 2015). For each wheat leaf sample, 30–50 infection sites from three leaves were examined to record the number of haustorial mother cells and haustoria, hyphal branches and hyphal length, and the hyphal infection area. All microscopic examinations were performed with an Olympus BX-51 microscope.

ACKNOWLEDGEMENTS

This study was supported by funds from the National Basic Research Program of China (No. 2013CB127700), the National Natural Science Foundation of China (No. 31371889) and the 111 Project from the Ministry of Education of China (No. B07049). The authors thank Professor Jinqiu Zhou (Institute of Biochemistry and Cell Biology, the Shanghai Institutes for Biological Sciences, Chinese Academy of Sciences, Shanghai, China) for providing technical support on the tetrad separation of yeast, and Professor Larry Dunkle (USDA-Agricultural Research Service at Purdue University, West Lafayette, IN, USA) for critical reading of the manuscript.

REFERENCES

Ayliffe, M., Devilla, R., Mago, R., White, R., Talbot, M., Pryor, A. and Leung, H. (2011) Nonhost resistance of rice to rust pathogens. *Mol. Plant–Microbe Interact.* **24**, 1143–1155.

Blackwell, E., Kim, H.J.N. and Stone, D.E. (2007) The pheromone-induced nuclear accumulation of the Fus3 MAPK in yeast depends on its phosphorylation state and on Dig1 and Dig2. *BMC Cell Biol.* **8**, 1–15.

Brefort, T., Müller, P. and Kahmann, R. (2005) The high-mobility-group domain transcription factor Rop1 is a direct regulator of *prf1* in *Ustilago maydis*. *Eukaryot. Cell*, **4**, 379–391.

Bruno, K.S., Tenjo, F., Li, L., Hamer, J.E. and Xu, J.R. (2004) Cellular localization and role of kinase activity of *PMK1* in *Magnaporthe grisea*. *Eukaryot. Cell*, **3**, 1525–1532.

Chang, Y.C., Wickes, B.L., Miller, G.F., Penoyer, L.A. and Kwon-Chung, K.J. (2000) *Cryptococcus neoformans STE12α* regulates virulence but is not essential for mating. *J. Exp. Med.* **191**, 871–882.

Chang, Y.C., Penoyer, L.A. and Kwon-Chung, K.J. (2001) The second *STE12* homologue of *Cryptococcus neoformans* is *MATa*-specific and plays an important role in virulence. *Proc. Natl. Acad. Sci. USA*, **98**, 3258–3263.

Chang, Y.C., Wright, L.C., Tscharke, R.L., Sorrell, T.C., Wilson, C.F. and Kwon-Chung, K.J. (2004) Regulatory roles for the homeodomain and C_2H_2 zinc finger regions of *Cryptococcus neoformans* Ste12αp. *Mol. Microbiol.* **53**, 1385–1396.

Chen, X.M. (2014) Integration of cultivar resistance and fungicide application for control of wheat stripe rust. *Can. J. Plant Pathol.* **36**, 311–326.

Cheng, Y.L., Wang, X.J., Yao, J.N., Voegele, R.T., Zhang, Y.R., Wang, W.M., Huang, L.L. and Kang, Z.S. (2015) Characterization of protein kinase *PsSRPKL*, a novel pathogenicity factor in the wheat stripe rust fungus. *Environ. Microbiol.* **17**, 2601–2617.

Chou, S., Lane, S. and Liu, H.P. (2006) Regulation of mating and filamentation genes by two distinct Ste12 complexes in *Saccharomyces cerevisiae*. *Mol. Cell. Biol.* **26**, 4794–4805.

Cuomo, C.A., Bakkeren, G., Khalil, H.B., Panwar, V., Joly, D., Linning, R., Sakthikumar, S., Song, X., Adiconis, X., Fan, L., Goldberg, J.M., Levin, J.Z., Young, S., Zeng, Q.D., Anikster, Y., Bruce, M., Wang, M.N., Yin, C.T., McCallum, B., Szabo, L.J., Hulbert, S., Chen, X.M. and Fellers, J.P. (2016) Comparative analysis highlights variable genome content of wheat rusts and divergence of the mating loci. *G3 (Bethesda)*, **7**, 361–376.

Eugenea, M., Kristian, K. and Mogenss, H. (2009) Evidence for increased aggressiveness in a recent widespread strain of *Puccinia striiformis* f. sp. *tritici* causing stripe rust of wheat. *Phytopathology*, **99**, 89–94.

Fields, S. and Herskowitz, I. (1985) The yeast *STE12* product is required for expression of two sets of cell-type specific genes. *Cell*, **42**, 923–930.

Fu, Y.P., Duan, X.Y., Tang, C.L., Li, X.R., Voegele, R.T., Wang, X.J., Wei, G.R. and Kang, Z.S. (2014) TaADF7, an actin-depolymerizing factor, contributes to wheat resistance against *Puccinia striiformis* f. sp. *tritici*. *Plant J.* **78**, 16–30.

Garnica, D.P., Upadhyaya, N.M., Dodds, P.N. and Rathjen, J.P. (2013) Strategies for wheat stripe rust pathogenicity identified by transcriptome sequencing. *PLoS One*, **8**, e67150.

Hamel, L.P. and Ellis, B.E. (2012) Mitogen-activated protein kinase signaling in plant-interacting fungi: distinct messages from conserved messengers. *Plant Cell*, **24**, 1327–1351.

Hartwell, L.H. (1980) Mutants of *Saccharomyces cerevisiae* unresponsive to cell division control by polypeptide mating hormone. *J. Cell Biol.* **85**, 811.

Hoi, J.W.S. and Dumas, B. (2010) Ste12 and Ste12-like proteins, fungal transcription factors regulating development and pathogenicity. *Eukaryot. Cell*, **9**, 480–485.

Hoi, J.W.S., Herbert, C., Bacha, N., O'Connell, R., Lafitte, C., Borderies, G., Rossignol, M., Rougé, P. and Dumas, B. (2007) Regulation and role of a STE12-like transcription factor from the plant pathogen *Colletotrichum lindemuthianum*. *Mol. Microbiol.* **64**, 68–82.

Holzberg, S., Brosio, P., Gross, C. and Pogue, G.P. (2002) Barley stripe mosaic virus-induced gene silencing in a monocot plant. *Plant J.* **30**, 315–327.

Ito, T. and Shinozaki, K. (2002) The *MALE STERILITY1* gene of Arabidopsis, encoding a nuclear protein with a PHD-finger motif, is expressed in tapetal cells and is required for pollen maturation. *Plant Cell Physiol.* **43**, 1285–1292.

Jin, Y., Szabo, L.J. and Carson, M. (2010) Century-old mystery of *Puccinia striiformis* life history solved with the identification of *Berberis* as an alternate host. *Phytopathology*, **100**, 432–435.

Johnson, A.D. (1995) Molecular mechanisms of cell-type determination in budding yeast. *Curr. Opin. Genet. Dev.* **5**, 552–558.

Kang, Z.S., Huang, L.L. and Buchenauer, H. (2002) Ultrastructural changes and localization of lignin and callose in compatible and incompatible interactions between wheat and *Puccinia striiformis*. *J. Plant Dis. Protect.* **109**, 25–37.

Kirkman-Correia, C., Stroke, I.L. and Fields, S. (1993) Functional domains of the yeast STE12 protein, a pheromone-responsive transcriptional activator. *Mol. Cell. Biol.* **13**, 3765–3772.

Kolmer, J.A. (2005) Tracking wheat rust on a continental scale. *Curr. Opin. Plant Biol.* **8**, 441–449.

Kramer, B., Thines, E. and Foster, A.J. (2009) MAP kinase signalling pathway components and targets conserved between the distantly related plant pathogenic fungi *Mycosphaerella graminicola* and *Magnaporthe grisea*. *Fungal Genet. Biol.* **46**, 667–681.

Lanchun, S., Bochu, W., Liancai, Z., Jie, L., Yanhong, Y. and Chuanren, D. (2003) The influence of low-intensity ultrasonic on some physiological characteristics of *Saccharomyces cerevisiae*. *Colloids Surf. B: Biointerfaces*, **30**, 61–66.

Li, C.X., Lin, H.Q. and Dubcovsky, J. (2015) Factorial combinations of protein interactions generate a multiplicity of florigen activation complexes in wheat and barley. *Plant J.* **84**, 70–82.

Li, D., Bobrowicz, P., Wilkinson, H.H. and Ebbole, D.J. (2005) A mitogen-activated protein kinase pathway essential for mating and contributing to vegetative growth in *Neurospora crassa*. *Genetics*, **170**, 1091–1104.

Line, R.F. (2002) Stripe rust of wheat and barley in North America: a retrospective historical review. *Annu. Rev. Phytopathol.* **40**, 75–118.

Liu, J., Guan, T., Zheng, P.J., Chen, L.Y., Yang, Y., Huai, B.Y., Li, D., Chang, Q., Huang, L.L. and Kang, Z.S. (2016) An extracellular Zn-only superoxide dismutase from *Puccinia striiformis* confers enhanced resistance to host-derived oxidative stress. *Environ. Microbiol.* **18**, 4118–4135.

Livak, K.J. and Schmittgen, T.D. (2001) Analysis of relative gene expression data using real-time quantitative PCR and the $2^{-\Delta\Delta}C_T$ method. *Methods*, **25**, 402–408.

Madhani, H.D. and Fink, G.R. (1997) Combinatorial control required for the specificity of yeast MAPK signaling. *Science*, **275**, 1314–1317.

Meng, X. and Zhang, S. (2013) MAPK cascades in plant disease resistance signaling. *Annu. Rev. Phytopathol.* **51**, 245–266.

Min, K., Shin, Y., Son, H., Lee, J., Kim, J.C., Choi, G.J. and Lee, Y.W. (2012) Functional analyses of the nitrogen regulatory gene *areA* in *Gibberella zeae*. *FEMS Microbiol. Lett.* **334**, 66–73.

Park, G., Xue, C.Y., Zheng, L., Lam, S. and Xu, J.R. (2002) *MST12* regulates infectious growth but not appressorium formation in the rice blast fungus *Magnaporthe grisea*. *Mol. Plant–Microbe Interact.* **15**, 183–192.

Park, G., Bruno, K.S., Staiger, C.J., Talbot, N.J. and Xu, J.R. (2004) Independent genetic mechanisms mediate turgor generation and penetration peg formation during plant infection in the rice blast fungus. *Mol. Microbiol.* **53**, 1695–1707.

Passmore, S., Maine, G.T., Elble, R., Christ, C. and Tye, B.K. (1989) *Saccharomyces cerevisiae* protein involved in plasmid maintenance is necessary for mating of *MATα* cells. *J. Mol. Biol.* **204**, 593–606.

Petty, I.T.D., French, R., Jones, R.W. and Jackson, A.O. (1990) Identification of barley stripe mosaic virus genes involved in viral RNA replication and systemic movement. *EMBO J.* **9**, 3453.

Rispail, N. and Di, P.A. (2009) *Fusarium oxysporum* Ste12 controls invasive growth and virulence downstream of the Fmk1 MAPK cascade. *Mol. Plant–Microbe Interact.* **22**, 830–839.

Rispail, N. and Pietro, A.D. (2010) The homeodomain transcription factor Ste12. *Commun. Integr. Biol.* **3**, 327–332.

Roelfs, A.P. and Bushnell, W.R. (1985) *The Cereal Rusts, Volume II: Diseases, Distribution, Epidemiology, and Control*. Orlando, FL: Academic.

Schamber, A., Leroch, M., Diwo, J., Mendgen, K. and Hahn, M. (2010) The role of mitogen-activated protein (MAP) kinase signalling components and the Ste12 transcription factor in germination and pathogenicity of *Botrytis cinerea*. *Mol. Plant Pathol.* **11**, 105–119.

Son, H., Seo, Y.S., Min, K., Park, A.R., Lee, J., Jin, J.M., Lin, Y., Cao, P.J., Hong, S.Y., Kim, E.K., Lee, S.H., Cho, A., Lee, S., Kim, M.G., Kim, Y., Kim, J.E., Kim, J.C., Choi, G.J., Yun, S.H., Lim, J.Y., Kim, M., Lee, Y.H., Choi, Y.D. and Lee, Y.W. (2011) A phenome-based functional analysis of transcription factors in the cereal head blight fungus, *Fusarium graminearum*. *PLoS Pathog.* **7**, e1002310.

Sprague, G.F. (1991) Assay of yeast mating reaction. *Methods Enzymol.* **194**, 77–93.

Tang, C.L., Wei, J.P., Han, Q.M., Liu, R., Duan, X.Y., Fu, Y.P., Huang, X.L., Wang, X.J. and Kang, Z.S. (2015) *PsANT*, the adenine nucleotide

translocase of *Puccinia striiformis*, promotes cell death and fungal growth. *Sci. Rep.* **5**, 11 241.

Tsuji, G., Fujii, S., Tsuge, S., Shiraishi, T. and Kubo, Y. (2003) The *Colletotrichum lagenarium* Ste12-like gene *CST1* is essential for appressorium penetration. *Mol. Plant–Microbe Interact.* **16**, 315–325.

Urban, M., Mott, E., Farley, T. and Hammond-Kosack, K. (2003) The *Fusarium graminearum MAP1* gene is essential for pathogenicity and development of perithecia. *Mol. Plant Pathol.* **4**, 347–359.

Vallim, M.A., Miller, K.Y. and Miller, B.L. (2000) *Aspergillus* SteA (sterile12-like) is a homeodomain-C^2/H^2-Zn^{+2} finger transcription factor required for sexual reproduction. *Mol. Microbiol.* **36**, 290–301.

Wang, C.F., Huang, L.L., Buchenauer, H., Han, Q.M., Zhang, H.C. and Kang, Z.S. (2007) Histochemical studies on the accumulation of reactive oxygen species (O_2^- and H_2O_2) in the incompatible and compatible interaction of wheat–*Puccinia striiformis* f. sp. *tritici*. *Physiol. Mol. Plant Pathol.* **71**, 230–239.

Wang, M.N. and Chen, X.M. (2013) First report of Oregon grape (*Mahonia aquifolium*) as an alternate host for the wheat stripe rust pathogen (*Puccinia striiformis* f. sp. *tritici*) under artificial inoculation. *Plant Dis.* **97**, 839.

Wellings, C.R. (2011) Global status of stripe rust: a review of historical and current threats. *Euphytica*, **179**, 129–141.

Yang, C., Liu, H.Q., Li, G.T., Liu, M.G., Yun, Y.Z., Wang, C.F., Ma, Z.H. and Xu, J.R. (2015) The MADS-box transcription factor FgMcm1 regulates cell identity and fungal development in *Fusarium graminearum*. *Environ. Microbiol.* **17**, 2762–2776.

Yin, C., Jurgenson, J.E. and Hulbert, S.H. (2011) Development of a host-induced RNAi system in the wheat stripe rust fungus *Puccinia striiformis* f. sp. *tritici*. *Mol. Plant–Microbe Interact.* **24**, 554–561.

Yuan, Y.L. and Fields, S. (1991) Properties of the DNA-binding domain of the *Saccharomyces cerevisiae* STE12 protein. *Mol. Cell. Biol.* **11**, 5910–5918.

Yuan, Y.O., Stroke, I.L. and Fields, S. (1993) Coupling of cell identity to signal response in yeast: interaction between the alpha 1 and STE12 proteins. *Gene Dev.* **7**, 1584–1597.

Yue, C.L., Cavallo, L.M., Alspaugh, J.A., Wang, P., Cox, G.M., Perfect, J.R. and Heitman, J. (1999) The STE12 alpha homolog is required for haploid filamentation but largely dispensable for mating and virulence in *Cryptococcus neoformans*. *Genetics*, **153**, 1601–1615.

Zhao, J., Wang, L., Wang, Z.Y., Chen, X.M., Zhang, H.C., Yao, J.N., Zhan, G.M., Chen, W., Huang, L.L. and Kang, Z.S. (2013) Identification of eighteen *Berberis* species as alternate hosts of *Puccinia striiformis* f. sp. *tritici* and virulence variation in the pathogen isolates from natural infection of barberry plants in China. *Phytopathology*, **103**, 927–934.

Zhao, J., Wang, M.N., Chen, X.M. and Kang, Z.S. (2016) Role of alternate hosts in epidemiology and pathogen variation of cereal rusts. *Phytopathology*, **54**, 207–228.

Zheng, W.M., Huang, L.L., Huang, J.Q., Wang, X.J., Chen, X.M., Zhao, J., Guo, J., Zhuang, H., Qiu, C.Z., Liu, J., Liu, H.Q., Huang, X.L., Pei, G.L., Zhan, G.M., Tang, C.L., Cheng, Y.L., Liu, M.J., Zhang, J.S., Zhao, Z.T., Zhang, S.J., Han, Q.M., Zhang, H.C., Zhao, J., Gao, X.N., Wang, J.F., Ni, P.X., Dong, W., Yang, L.F., Yang, H.M., Xu, J.R., Zhang, G.Y. and Kang, Z.S. (2013) High genome heterozygosity and endemic genetic recombination in the wheat stripe rust fungus. *Nat. Commun.* **5**, 2673.

Zhou, X.Y., Liu, W.D., Wang, C.F., Xu, Q.J., Wang, Y., Ding, S.L. and Xu, J.R. (2011) A MADS-box transcription factor MoMcm1 is required for male fertility, microconidium production and virulence in *Magnaporthe oryzae*. *Mol. Microbiol.* **80**, 33–53.

SUPPORTING INFORMATION

Additional Supporting Information may be found in the online version of this article at the publisher's website:

Fig. S1 Multi-sequence alignment and phylogenetic analysis of PstSTE12 and other orthologues of STE12 in other species. (A) Alignment showing the identity of STE12 homeodomains of *Puccinia striiformis* f. sp. *tritici* (*Pst*). Bold overlines mark the three helices of the homeodomain. Solid underline indicates the conserved tryptophan and phenylalanine residues of Helix III known to be essential for DNA binding. (B) Phylogeny of fungal *STE12* orthologues. The phylogenetic tree was constructed using the maximum-likelihood (ML) approach. The confidence level for the groupings was estimated using 500 bootstrap replicates. The numbers adjacent to the branch points indicate the percentage of replicates supporting each branch. Scale bars correspond to 0.1 amino acid substitutions.

Fig. S2 Two C_2/H_2-Zn^{2+} finger domains of the C-terminal region were predicted in PstSTE12 via the National Center for Biotechnology Information (NCBI).

Fig. S3 Tetrads were separated from the ascospores formed by the diploid mutant after cultivation in MacConkey medium. Four viable spores (A–D) were obtained from each of the tetrads (lanes 1, 3, 6–10 and 12) with some exceptions of two- or three-spore tetrads as a result of random spore inviability (lanes 2, 4, 5 and 11).

Fig. S4 Sequence regions for the host-induced gene silencing (HIGS) and quantitative reverse transcription-polymerase chain reaction (qRT-PCR) experiments in this study. Black arrows indicate the start codon, HIGS targeted sites, qRT-PCR site and stop codon. The numbers in parentheses indicate the distance to the start codon (ATG). The sequences of the two domains are labelled in grey.

Table S1 Primers used for the assays in this study.